A Singlet Biradicaloid Zinc Compound and Its Nonradical Counterpart

ARTICLE *in* JOURNAL OF THE AMERICAN CHEMICAL SOCIETY · APRIL 2013

Impact Factor: 12.11 · DOI: 10.1021/ja402351x · Source: PubMed

7 AUTHORS, INCLUDING:

Amit Pratap Singh
Georg-August-Universität Göttingen
19 PUBLICATIONS **305** CITATIONS
SEE PROFILE

Herbert W Roesky
Gesellschaft für wissenschaftliche Datenvera…
782 PUBLICATIONS **13,622** CITATIONS
SEE PROFILE

Martin Schwarzer
Ibaraki University
15 PUBLICATIONS **233** CITATIONS
SEE PROFILE

Birger Dittrich
Heinrich-Heine-Universität Düsseldorf
189 PUBLICATIONS **2,426** CITATIONS
SEE PROFILE

JACS
JOURNAL OF THE AMERICAN CHEMICAL SOCIETY
Article
pubs.acs.org/JACS

A Singlet Biradicaloid Zinc Compound and Its Nonradical Counterpart

Amit Pratap Singh,[†] Prinson P. Samuel,[†] Herbert W. Roesky,*[,†] Martin C. Schwarzer,[‡] Gernot Frenking,*[,‡] Navdeep S. Sidhu,[†] and Birger Dittrich*[,§]

[†]Institut für Anorganische Chemie, Georg-August-Universität, Tammannstraße 4, 37077 Göttingen, Germany
[‡]Fachbereich Chemie, Philipps-Universität Marburg, Hans-Meerweinstraße, 35032 Marburg, Germany
[§]Institut für Anorganische und Angewandte Chemie, Universität Hamburg, Martin-Luther-King-Platz 6, 20146-Hamburg, Germany

Supporting Information

ABSTRACT: Metal ions with radical centers in their coordination sphere are key participants in biological and catalytic processes. In the present study, we describe the synthesis of the cAAC:$ZnCl_2$ adduct (**1**) using a cyclic alkylaminocarbene (cAAC) as donor ligand. Compound **1** was treated with 2 equiv of KC_8 and $LiB(sec\text{-}Bu)_3H$ to yield a deep blue-colored dicarbene zinc compound $(cAAC)_2Zn$ (**2**) and the colorless hydrogenated zinc compound $(cAACH)_2Zn$ (**3**), respectively. Compounds **2** and **3** were well characterized by spectroscopic methods and single-crystal X-ray structural analysis. Density functional theory calculations were performed for **2** which indicate that this molecule possesses a singlet biradicaloid character. Moreover, we show the application of **2** in CO_2 activation, which yields a zwitterionic cAAC·CO_2 adduct.

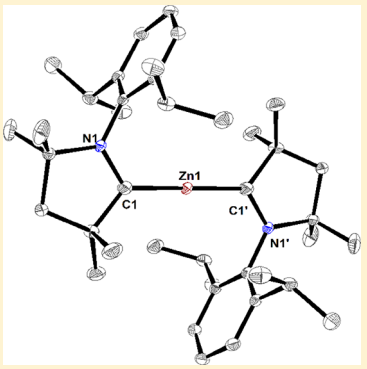

INTRODUCTION

Radicals and biradicals are very reactive chemical species that play important roles in combustion, atmospheric chemistry, plasma and polymerization chemistry, biochemistry, and a number of other chemical processes.[1] Metal ions with radical centers in their coordination sphere are key participants in biological and catalytic radical processes.[2] There are a few examples reported in the literature on the synthesis of metal ions with a radical center in their coordination sphere by using an organic ligand with a radical center or incorporating an *in situ*-generated radical species.[3] In 2007, Fedushkin and co-workers[4] reported on the synthesis and characterization of a biradical dizinc compound supported by a radical anionic ligand, 1,2-bis[(2,6-diisopropylphenyl)imino]acenaphthene (dpp-Bian). The dpp-Bian is bound to zinc in a bidentate mode, resulting in a five-membered chelate ring. A similar type of bonding was observed previously by Raston and co-workers[5] for the 1,4-di-*tert*-butyl-1,4-diazabutadiene ligand with magnesium and zinc. These compounds were found to be triplets in their ground state. However, a singlet biradical of two-coordinated zinc is still elusive. In this context, we have established a completely different approach for the synthesis of a singlet biradical two-coordinated zinc compound, $(cAAC)_2Zn$ (**2**), using a cyclic alkylaminocarbene (cAAC).[6] So far no physical methods are available to characterize unambiguously the biradicaloid status of such compounds, and this prompted us to synthesize also a nonradical counterpart, $(cAACH)_2Zn$ (**3**), of the biradicaloid zinc compound **2** (Scheme 1).

Furthermore, we show the application of **2** in CO_2 activation. The coordination of CO_2, its activation, and its conversion into organic compounds are rapidly growing domains of coordination chemistry, organometallic chemistry, and catalysis.[7] Most of the literature reports indicate that activation of CO_2 requires high temperature, or at least room temperature, and often the presence of an activator or catalyst.[8] In this respect, CO_2 activation at lower temperature merits attention. Compound **2** activates CO_2 at −30 °C within a few minutes to give a zwitterionic cAAC·CO_2 (**4**) adduct. Furthermore, **4** acts as a stable cAAC source which eliminates CO_2 in the presence of zinc dichloride. Such a reversible fixation of CO_2, which has so far been observed only in polymers bearing N-bases,[9] offers an exciting challenge for further investigations in the context of environmental chemistry.

RESULTS AND DISCUSSION

Synthesis. Compounds **2** and **3** were each synthesized in two steps. In the first step, 2 equiv of cAAC were treated with 1 equiv of $ZnCl_2$ in THF to give a 1:1 adduct of cAAC:$ZnCl_2$ (**1**); 1 equiv of carbene remained unreactive. In the second step, the reaction mixture was treated with 2 equiv of KC_8 at −78 °C. A deep blue color appeared in the solution at −50 °C. After 1 h of stirring, the reaction mixture was filtered, and the filtrate was stored for 1 day at −4 °C to give deep blue crystals of **2**. However, the reaction mixture of **1** and cAAC with

Received: March 6, 2013

   dx.doi.org/10.1021/ja402351x | J. Am. Chem. Soc. XXXX, XXX, XXX−XXX

Scheme 1. Synthesis of Compounds 1−4

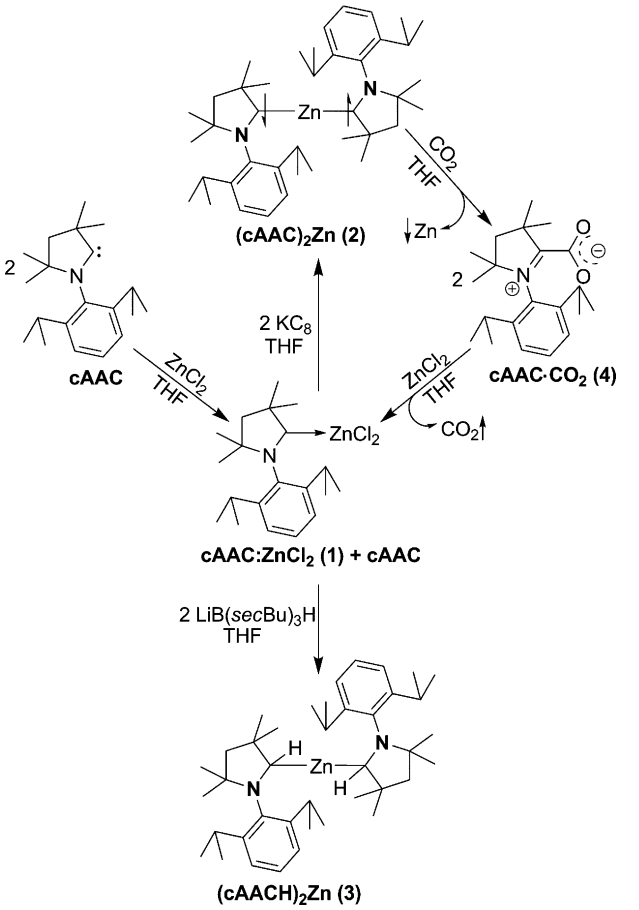

$LiB(sec\text{-}Bu)_3H$ yielded a colorless clear solution at room temperature. After removal of the solvent, a colorless solid of **3** was obtained. The crude compound was purified by crystallization. Single crystals suitable for X-ray diffraction analysis of **3** were obtained from a concentrated toluene solution at −32 °C. In an alternative route for the synthesis of **2**, we reacted cAAC and $ZnCl_2$ in a 1:1 ratio to prepare the cAAC:$ZnCl_2$ adduct **1**, and this adduct was then treated with cAAC and KC_8 in a ratio of 1:2.1 to give **2**. In another experiment, when CO_2 was bubbled through the THF solution of **2** at −30 °C for 2−3 min, an immediate color change from blue to light yellow was observed. The concentrated THF solution gave colorless crystals of **4** at −4 °C. In the literature it is reported that R_2Zn compounds do not react with CO_2 at room temperature, especially in the absence of a catalyst.[10] In contrast, **2** reacts rapidly at −30 °C. We assume that, due to the presence of radical centers at the "carbene" carbon atoms in **2**, CO_2 is easily activated to give the stable cAAC·CO_2 adduct **4** as a colorless compound. We observed that cAAC does not react with CO_2 at −30 °C, but reacts very slowly at 25−30 °C to give **4**. Furthermore, **3** does not react with CO_2 even at higher temperatures up to 50 °C. These experiments clearly indicate that the biradicaloid nature of **2** promotes CO_2 activation even at low temperatures. Compounds **2**−**4** have been fully characterized by elemental analysis, various spectroscopic methods, and single-crystal X-ray structural analysis. The UV−visible absorption maximum for the intensely blue-colored THF solution of **2** appeared at 630 nm. However, **2** was found to be electron paramagnetic resonance (EPR) silent, and it showed quite sharp resonances in its ^1H NMR spectrum with slightly different positions in comparison with those of the free carbene cAAC and **3**. In addition, **3** showed a singlet resonance in its ^1H NMR spectrum at 3.34 ppm for C*H*−Zn protons. ^{13}C NMR spectra of **2** and **3** exhibited resonances for the "carbene" carbon at 151 ppm ($C^{\bullet}$−Zn) and 78 ppm (CH−Zn), respectively. In the FT-IR spectrum of **4**, the $\nu(CO_2)$ vibrations were observed at 1666 and 1610 cm^{-1}.

Crystal Structure Analysis. In order to establish unambiguously the structural features of **2**−**4**, single-crystal X-ray structural analysis were carried out. The crystal and structure refinement parameters for **2**−**4** are given in Table S1 (Supporting Information). The molecular structures of **2** and **3** show that these compounds are analogues of the R_2Zn compounds (e.g., dimethylzinc and diethylzinc). The latter are very important reagents in various organic and inorganic transformations.[11] Under standard conditions both dimethylzinc and diethylzinc exist as volatile, pyrophoric liquids (Me_2Zn: mp −42 °C, bp 46 °C; Et_2Zn: mp −28 °C, bp 118 °C). Recently Steiner and co-workers[12] reported the crystal structures of Me_2Zn and Et_2Zn which exhibit a rich solid-phase behavior. The solid-state studies of diarylzinc and bulky dialkylzinc derivatives revealed that these molecules exhibit monomeric structures.[13] The crystal structures of **2** and **3** show that the zinc atom is covalently bound to the two cAAC molecules, resulting in a linear geometry as observed in the case of Me_2Zn and Et_2Zn. The C1−Zn1 bond length in **2** is 1.8850(17) Å, which is shorter than the corresponding bond lengths found in **3** (2.041(4) Å) and Me_2Zn (1.927(6) Å).[12] The C1−Zn1−C1′ bond angles in both **2** and **3** are 180.0°; the zinc atom is found in the inversion center (Figures 1 and 2). In

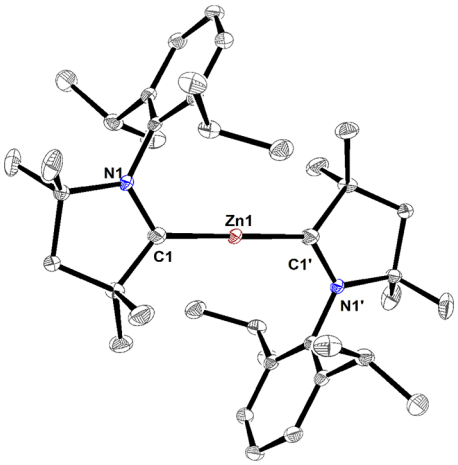

Figure 1. Molecular structure of **2**. H atoms are omitted for clarity. Anisotropic displacement parameters are depicted at the 50% probability level. Selected experimental [calculated at RI-BP86/def2-SVP singlet; triplet; singlet biradical] bond lengths [Å] and angles [°]: Zn1−C1 1.8850(17) [1.896; 1.924; 1.902], C1− N1 1.376(2) [1.388; 1.398; 1.392], C1−C1′3.770 [3.791; 3.851; 3.805], C1−Zn1−C1′ 180.0 [180.0; 177.6; 180.0].

2 and **3** the geometry around the "carbene" carbon atom is trigonal planar and distorted tetrahedral, respectively. This geometric difference between **2** and **3** unambiguously shows the presence of the hydrogen atom at the "carbene" carbon of the latter. The shorter C−Zn bond length of **2** is further explained by the density functional theory (DFT) calculations. The crystal structure of the reaction product **4**, shown in Figure

dx.doi.org/10.1021/ja402351x | J. Am. Chem. Soc. XXXX, XXX, XXX−XXX

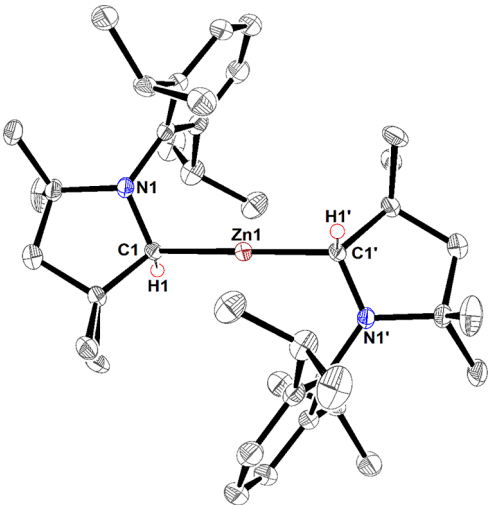

Figure 2. Molecular structure of **3**. H atoms (except C*H*−Zn) and solvent molecules are omitted for clarity. Anisotropic displacement parameters are depicted at the 50% probability level. Selected experimental [calculated at RI-BP86/def2-SVP singlet] bond lengths [Å] and angles [°]: C1−Zn1 2.041(4) [2.014], C1−N1 1.457(6) [1.472], C1−Zn−C1′ 180.0 [179.9].

3, exhibits a zwitterionic bonding state. The nearly equivalent C−O bond distances (1.2395(19) and 1.2352(19) Å) indicate that the negative charge is delocalized equally among the central carbon (C21) and the two oxygen (O1 and O2) atoms. In contrast, the C1−N1 bond distance (1.2920(18) Å) is substantially shorter than 1.376(2) Å as found in the parent compound **2**. This indicates a double bond character between C1 and N1 atoms resulting in a formal positive charge at the nitrogen atom in **4**. The C1−C21 bond length (1.521(2) Å) is longer than those reported for analogous zwitterionic CO_2 adducts,[8c] which indicates that CO_2 is only loosely bound to cAAC. Therefore, treatment of **3** with even 0.5 equiv of $ZnCl_2$ results in the elimination of CO_2 to give a 1:1 mixture of **1** and cAAC, which can be further used to obtain **2**, thus completing the cycle (Scheme 1). Moreover, **4** is quite stable for long period of time under an inert atmosphere and does not release CO_2.

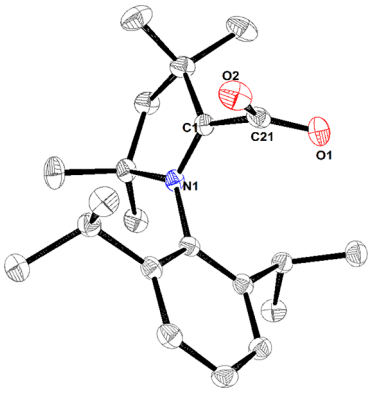

Figure 3. Molecular structure of **4**. H atoms are omitted for clarity. Anisotropic displacement parameters are depicted at the 50% probability level. Selected experimental [calculated at RI-BP86/def2-SVP singlet] bond lengths [Å] and angles [°]: C1−C21 1.521(2) [1.520], C1−N1 1.2920(18) [1.323], C21−O1 1.2395(19) [1.262], C21−O2 1.2352(19) [1.241], O1−C21−O2 131.41(14) [131.4].

DFT Calculations for Compounds 2−4. Compound **2** exhibits no EPR resonance, suggesting a closed-shell ground state of **2**. In order to gain more insight into the electronic situation of **2**, DFT calculations were performed for the geometries of the singlet and triplet states at the RI-BP86/def2-SVP level of theory.[14,23,24] The bond lengths and angles of **2** depicted in the legend of Figure 1 illustrate that the calculated values for the singlet biradical are in better agreement with the experimental values when compared with those of the superposition of the X-ray structure with the calculated singlet and triplet forms (Supporting Information). The experimental structure shows a nearly perfect alignment with the singlet form, while the calculated triplet exhibits a significantly greater deviation. Calculations at the RI-BP86/def2-TZVPP//def2-SVP level predict that the singlet is 6.9 kcal/mol lower in energy than the triplet, whereas the singlet biradical is 0.1 kcal/mol below the closed-shell singlet. The DFT calculations using the functionals M05-2X, B3LYP, and PBE0 suggest that the triplet state of **2** is slightly lower in energy than the closed-shell singlet but the singlet biradical form is always more stable than the triplet state (Table S2, Supporting Information). Thus, the calculations agree with the conclusion reached from the EPR analysis that **2** is not a triplet biradical. At the same time the DFT calculations also suggest that the molecule possesses biradicaloid character. This is supported by a CASSCF[2,2]/def2-SVP calculation of **2** which gives coefficients of 0.81 and −0.59 for the ground and first excited configurations. Figure 4a,b shows the highest lying degenerate singly occupied

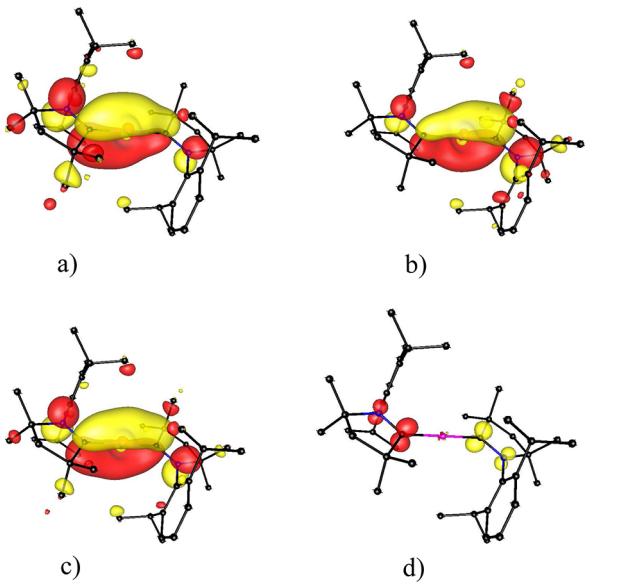

Figure 4. (a,b) Plots of the highest lying degenerate SOMOs of the singlet biradical state of **2**. (c) Plots of the HOMO of the closed-shell singlet state of **2**. (d) Plot of the spin density of the singlet biradical state **2**. All calculations at the RI-BP86/def2-TZVPP//def2-SVP level.

molecular orbitals (SOMOs) of the singlet biradical state of **2**. The π-type orbitals are polarized toward either carbon atom. The highest occupied molecular orbital (HOMO) of the closed-shell singlet state of **2** is symmetric with respect to the two ligands (Figure 4c). The calculated spin density of the singlet biradical state of **2** (Figure 4d) indicates that the unpaired electrons are mainly located at the carbon donor atoms of the ligands and to a minor extent at the nitrogen atoms.

dx.doi.org/10.1021/ja402351x | J. Am. Chem. Soc. XXXX, XXX, XXX−XXX

The bonding situation in **2** and the preference for a singlet biradicaloid structure can thus be explained as follows. The C−Zn σ bonds come from electron-sharing interactions between the unpaired electrons in the σ orbitals of the carbene carbon atom of the cAAC ligands in the triplet state and Zn (Figure 5).

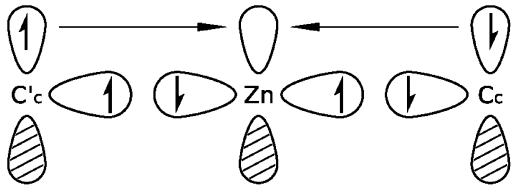

Figure 5. Schematic representation of the chemical bonding between Zn and the carbon atoms in the singlet biradical state of **2**. The σ orbital at Zn sketches the two lobes of the sp hybrids which point toward the carbon atoms.

The use of the excited triplet state of the ligands as reference state is supported by the finding that the HOMO of **2** is a π orbital. Electron-sharing bonds are much stronger than donor−acceptor bonds, which compensate for the singlet−triplet excitation energy of the ligands. A similar situation was recently found for the Si−C bonding in $(cAAC)_2SiCl_2$.[18] The unpaired π electrons at the carbene carbon atom couple via the vacant p(π) atomic orbital of Zn which receives an equal amount of α and β electrons from the ligands. Therefore, the spin density rests on the carbene carbon atom with small contributions at the nitrogen lone pair orbital which couple with the unpaired electrons.

We also optimized the geometries of **3** and **4**. Theoretical values for bond lengths and angles are in very good agreement with the experiment (Figures 2 and 3 and Supporting Information). It is noteworthy that the calculated C1−N1 bond length increases from **4** (1.323 Å) to **2** (1.392 Å) and **3** (1.472 Å) which is in accord with the experimental values. It indicates that the N1→C1 π interaction which is quite strong in **4**, but negligible in **3**, plays an intermediate role in the π conjugation and thus in the stabilization of the biradicaloid species. This is supported by the shape of the SOMO (which are N1−C1 antibonding) and the energetically lower lying doubly occupied π orbitals (which are N1−C1 bonding) that have quite large coefficients at N1. The Wiberg bond order for the N1−C1 bond for **4** is 1.48, for **2** is 1.15, and for **3** is 0.97, giving numerical evidence for the strength of the partial π bonding in the molecules. According to the RI-BP86/def2-TZVPP//RI-BP86/def2-SVP calculations, the hydrogenation of **2** yielding **3** is exergonic by −36.7 kcal/mol. The bond strength of the cAAC−CO_2 complex is calculated at the same level of theory to be 15.8 kcal/mol.

CONCLUSION

We have developed novel methodologies for the synthesis of singlet biradicaloid dicarbene zinc compound **2**. The biradicaloid nature of the compound was proven by the synthesis of a nonradical counterpart **3**. The biradicaloid zinc compound has shorter C−Zn bond lengths than the nonradical counterpart due to the strong back-bonding. DFT calculations for **2** indicate that this molecule possesses a singlet biradicaloid character. We have also shown that such a zinc centered singlet biradicaloid activates CO_2 at low temperature. A comparison of the C−Zn bond lengths of 1.927 Å for Me_2Zn and 1.885 Å for $(cAAC)_2Zn$ indicates that a shorter C−Zn bond in the latter is even more reactive than the longer one when both react with CO_2. The difference in the reaction temperature is more than 80 °C.[10] This result leads us to assume that a singlet biradicaloid system could be an important reagent for various other chemical processes. Such investigations will be reported in due course from our laboratory.

EXPERIMENTAL SECTION

All reactions and handling of reagents were performed under an atmosphere of dry nitrogen or argon using standard Schlenk techniques or a glovebox where the O_2 and H_2O levels were usually kept below 1 ppm. The cyclic alkylaminocarbene (cAAC) was synthesized following a reported procedure.[6] Solvents were purified with the M-Braun solvent drying system. Solution NMR spectra were recorded on Bruker Avance 200, Bruker Avance 300, and Bruker Avance 500 MHz NMR spectrometers. Elemental analyses were performed by the Analytisches Labor des Instituts für Anorganische Chemie der Universität Göttingen. Melting points were measured in sealed glass tubes on a Büchi B-540 melting point apparatus.

Synthesis of cAAC:$ZnCl_2$ (1). Tetrahydrofuran (30 mL) was cooled to −50 °C and added to a 1:1 mixture of cAAC (3.50 mmol, 1.00 g) and $ZnCl_2$ (3.50 mmol, 478 mg). The reaction mixture was slowly warmed to room temperature and stirred for 3 h. A white precipitate appeared which was then filtered over a frit and dried under vacuum to obtain pure **1**: yield 1.18 g, 80%; mp 194−195 °C; ^{1}H NMR (CD_3CN, 298 K, 500 MHz, δ ppm) 7.48−7.45 (m, $1H_{ar}$, *p-H*), 7.38−7.37 (d, $2H_{ar}$, *m-H*), 2.85−2.80 (m, 2H, C*H*Me_2), 2.14 (s, 2H, CH_2), 1.51 (s, 6H, CH_3), 1.41 (s, 6H, CH_3), 1.31−1.29 (m, 12H, CHCH_3); ^{13}C NMR (CD_3CN, 298 K, 126 MHz, δ ppm) 146.7, 135.2, 133.o, 131.1, 126.4, 56.8, 50.1, 30.2, 29.8, 29.4, 28.8, 26.2, 22.1. Elemental analysis, found (calcd) for $C_{20}H_{31}Cl_2NZn$: C, 56.31 (56.95); H, 7.21 (7.41); N, 3.16 (3.32).

Synthesis of $(cAAC)_2Zn$ (2). Tetrahydrofuran (50 mL) was cooled to −78 °C and added to a 1:1:2.1 mixture of **1** (2.37 mmol, 1.00 g), cAAC (2.37 mmol, 676 mg), and KC_8 (4.97 mmol, 672 mg) while stirring. The reaction mixture was slowly warmed to room temperature and stirred for an additional hour to give a deep blue solution. The solution was then filtered, and the volume of the filtrate was reduced to half and stored at −4 °C to give blue crystals suitable for single-crystal X-ray analysis of **2**: yield 1.17 g, 78%; mp 175−180 °C; UV/vis λ_{ab} = 630 nm; ^{1}H NMR (THF-d_8, 298 K, 500 MHz, δ ppm) 7.19−7.18 (m, $2H_{ar}$, *p-H*), 7.12−7.11 (d, $4H_{ar}$, *m-H*), 3.26−3.23 (m, 4H, C*H*Me_2), 1.88 (s, 4H, CH_2), 1.38 (d, 12H, CHCH_3), 1.29 (s, 12H, CH_3), 1.19 (d, 12H, CHCH_3), 0.84 (s, 12H, CH_3); ^{13}C NMR (THF-d_8, 298 K, 126 MHz, δ ppm) 151.2, 139.4, 130.2, 128.1, 126.2, 69.7, 56.9, 47.5, 34.0, 30.6, 30.4, 30.1, 29.9, 28.9. Elemental analysis, found (calcd) for $C_{40}H_{62}N_2Zn$: C, 74.15 (75.50); H, 10.16 (9.82); N, 4.29 (4.40).

Synthesis of $(cAACH)_2Zn$ (3). Tetrahydrofuran (50 mL) was added to a 1:1 mixture of **1** (2.37 mmol, 1.00 g) and cAAC (2.37 mmol, 676 mg). The reaction mixture was cooled to −78 °C, and LiB(*sec*-Bu)$_3$H in THF (1 M, 4.74 mmol, 4.74 mL) was added slowly with stirring. The reaction mixture was warmed to room temperature and stirred for an additional 10 min to give a colorless solution. The volatiles were removed under reduced pressure to obtain a colorless solid. The crude solid was then dissolved in toluene and stored at −32 °C to give colorless crystals of **3** suitable for single-crystal X-ray analysis: yield 1.21 g, 80%; mp 169−173 °C; ^{1}H NMR (THF-d_8, 298 K, 500 MHz, δ ppm) 7.17−7.14 (m, $2H_{ar}$, *p-H*), 7.12−6.90 (m, $4H_{ar}$, *m-H*), 4.26−4.23 (m, 4H, C*H*Me_2), 3.34 (s, 2H, C*H*-Zn), 1.50 (s, 4H, CH2), 1.25 (d, 12H, CHCH_3), 1.06 (d, 12H, CHCH_3), 0.90 (s, 12H, CH_3), 0.50 (s, 12H, CH_3); ^{13}C NMR (THF-d_8, 298 K, 126 MHz, δ ppm) 140.9, 129.6, 127.2, 125.6, 78.2, 65.4, 52.9, 45.3, 33.1, 32.6, 29.4, 28.1, 27.9, 24.5. Elemental analysis, found (calcd) for $C_{54}H_{80}N_2Zn$: C, 78.48 (78.84); H, 9.56 (9.80); N, 3.53 (3.41).

Synthesis of cAAC·CO_2 (4). CO_2 was passed over a tetrahydrofuran solution (50 mL) of **2** (0.78 mmol, 500 mg) at −30 °C for 2−3 min. An immediate color change of the solution was observed from blue to light yellow with little turbidity. The latter was

dx.doi.org/10.1021/ja402351x | J. Am. Chem. Soc. XXXX, XXX, XXX−XXX

characterized as Zn metal by elemental analysis. The reaction mixture was then filtered through a frit, and the filtrate was stored at −4 °C to give colorless needle-shaped crystals of **4**: yield 450 mg, 87%; mp 182−185 °C; ^{1}H NMR (THF-d_8, 298 K, 500 MHz, δ ppm) 7.39−7.27 (m, 3H$_{ar}$), 2.89−2.76 (m, 2H, C*H*Me$_2$), 2.30 (s, 2H, CH_2), 1.59 (s, 6H, CH_3), 1.46 (s, 6H, CH_3), 1.33−1.27 (m, 12H, CHCH_3); ^{13}C NMR (THF-d_8, 298 K, 126 MHz, δ ppm) 195.1, 157.7, 147.1, 135.1, 130.9, 126.1, 50.3, 48.2, 30.6, 30.4, 29.2, 28.9; FT-IR (KBr) ν(CO$_2$) 1666 and 1610 cm^{-1}. Elemental analysis, found (calcd) for $C_{21}H_{31}NO_2$: C, 75.84 (76.55); H, 9.62 (9.48); N, 4.08 (4.25).

Crystal Structure Determination. Molecular structures of **2**−**4** were established by single-crystal X-ray crystallographic studies, and the corresponding ORTEP representations are shown in Figures 1−3. Crystals were measured on a Bruker three-circle diffractometer equipped with a SMART 6000 CCD area detector and a Cu Kα rotating anode. Integrations were performed with SAINT.[19] Intensity data for all compounds were corrected for absorption and scaled with SADABS.[20] Structures were solved by direct methods and initially refined by full-matrix least-squares methods on F^2 with the program SHELXL-97,[21] utilizing anisotropic displacement parameters for non-hydrogen atoms. Visualization and modeling were done using SHELXLE.[22]

Computational Details. Geometry optimizations were carried out using the DFT functionals BP86,[14] (for **2**−**4**) M05-2X,[15] B3LYP,[16] and PBE0[17] (all for **2**) with def2-SVP basis sets.[23] The RI approximation was applied whenever possible.[24] The optimized geometries were verified as minima on the potential energy surface by calculation of the vibrational frequencies analytically (AO-FORCE).[25] Improved energies were calculated with the larger basis sets def2-TZVPP[26] using geometries obtained with the SVP basis set. Calculations were carried out with the program packages Gaussian09[27] and Turbomole 6.3.[28]

■ ASSOCIATED CONTENT

Ⓢ Supporting Information

Crystallographic data (CIF), details of DFT calculations, and complete ref 27. This material is available free of charge via the Internet at http://pubs.acs.org.

■ AUTHOR INFORMATION

Corresponding Author

hroesky@gwdg.de; frenking@chemie.uni-marburg.de; bdittri@gwdg.de and birger.dittrich@chemie.uni-hamburg.de

Notes

The authors declare no competing financial interest.

■ ACKNOWLEDGMENTS

H.W.R. thanks the Deutsche Forschungsgemeinschaft (DFG RO 224/60-1) for financial support.We are thankful to Dr. A. Claudia Stückl for EPR measurements. N.S.S. thanks Prof. George M. Sheldrick for help in the refinement of structure **3**.

■ REFERENCES

(1) (a) Smith, M. B.; March, J. *Advanced Organic Chemistry*, 5th ed.; Wiley, New York, 2001; (b) Gavrilescu, M.; Chisti, Y. *Biotechnol. Adv.* **2005**, *23*, 471−499. (c) Valko, M.; Rhodes, C. J.; Moncol, J.; Izakovic, M.; Mazur, M. *Chem.-Biol. Interact.* **2006**, *160*, 1−40. (d) Hayesa, C. J.; Merleb, J. K.; Hadad, C. M. *Adv. Phys. Org. Chem.* **2009**, *43*, 79−134. (e) Glowacki, D. R.; Pilling, M. J. *ChemPhysChem* **2010**, *11*, 3836−3843. (f) Vázquez-Dorbatt, V.; Lee, J.; Lin, E.-W.; Maynard, H. D. *ChemBioChem* **2012**, *13*, 2478−2487. (g) Chu, D. S. H.; Schellinger, J. G.; Shi, J.; Convertine, A. J.; Stayton, P. S.; Pun, S. H. *Acc. Chem. Res.* **2012**, *45*, 1089−1099.

(2) Andreini, C.; Bertini, I.; Cavallaro, G.; Holliday, G. L.; Thornton, J. M. *J. Biol. Inorg. Chem.* **2008**, *13*, 1205−1208.

(3) (a) Felthouse, T. R.; Dong, T.-Y.; Hendrickson, D. N.; Shieh, H.-S.; Thompson, M. R. *J. Am. Chem. Soc.* **1986**, *108*, 8201−8214. (b) Mack, J.; Stillman, M. J. *J. Am. Chem. Soc.* **1994**, *116*, 1292−1304. (c) Vangberg, T.; Lie, R.; Ghosh, A. *J. Am. Chem. Soc.* **2002**, *124*, 8122−8130. (d) Ishii, N.; Okamura, Y.; Chiba, S.; Nogami, T.; Ishida, T. *J. Am. Chem. Soc.* **2008**, *130*, 24−25. (e) Scepaniak, J. J.; Wright, A. M.; Lewis, R. A.; Wu, G.; Hayton, T. W. *J. Am. Chem. Soc.* **2012**, *134*, 19350−19353.

(4) Fedushkin, I. L.; Skatova, A. A.; Ketkov, S. Y.; Eremenko, O. V.; Piskunov, A. V.; Fukin, G. K. *Angew. Chem.* **2007**, *119*, 4380−4383; *Angew. Chem., Int. Ed.* **2007**, *46*, 4302−4305.

(5) Gardiner, M. G.; Hanson, G. R.; Henderson, M. J.; Lee, F. C.; Raston, C. L. *Inorg. Chem.* **1994**, *33*, 2456−2461.

(6) Lavallo, V.; Canac, Y.; Präsang, C.; Donnadieu, B.; Bertrand, G. *Angew. Chem.* **2005**, *117*, 5851−5855; *Angew. Chem., Int. Ed.* **2005**, *44*, 5705−5709.

(7) (a) Yin, X.; Moss, J. R. *Coord. Chem. Rev.* **1999**, *181*, 27−59. (b) Myers, T. W.; Berben, L. A. *Chem. Commun.* **2013**, *49*, 4175−4177.

(8) (a) Villiers, C.; Dognon, J.-P.; Pollet, R.; Thuéry, P.; Ephritikhine, M. *Angew. Chem.* **2010**, *122*, 3543−3546; *Angew. Chem., Int. Ed.* **2010**, *49*, 3465−3468. (b) Kuchenbeiser, G.; Soleilhavoup, M.; Donnadieu, B.; Bertrand, G. *Chem. Asian J.* **2009**, *4*, 1745−1750. (c) Duong, H. A.; Tekavec, T. N.; Arif, A. M.; Louie, J. *Chem. Commun.* **2004**, 112−113.

(9) (a) Ochiai, B.; Yokota, K.; Fujii, A.; Nagai, D.; Endo, T. *Macromolecules* **2008**, *41*, 1229−1236. (b) Vogiatzis, K. D.; Mavrandonakis, A.; Klopper, W.; Froudakis, G. E. *Chem. Phys. Chem.* **2009**, *10*, 374−383. (c) Patel, H. A.; Je, S. H.; Park, J.; Chen, D. P.; Jung, Y.; Yavuz, C. T.; Coskun, A. *Nat. Commun.* **2013**, *4*, 1357.

(10) Boersma, J. In *Comprehensive Organometallic Chemistry*; Wilkinson, G., Stone, F. G. A., Abel, E. W., Eds.; Pergamon Press: Oxford, 1982; Vol. 2, p 850.

(11) (a) Erdik, E. *Organozinc Reagents in Organic Synthesis*; CRC Press: Boca Raton, FL, 1996. (b) Pu, L.; Yu, H.-B. *Chem. Rev.* **2001**, *101*, 757−824.

(12) Bacsa, J.; Hanke, F.; Hindley, S.; Odedra, R.; Darling, G. R.; Jones, A. C.; Steiner, A. *Angew. Chem.* **2011**, *123*, 11889−11891; *Angew. Chem., Int. Ed.* **2011**, *50*, 11685−11687.

(13) (a) Haaland, A.; Green, J. C.; McGrady, G. S.; Downs, A. J.; Gullo, E.; Lyall, M. J.; Timberlake, J.; Tutukin, A. V.; Volden, H. V.; Østby, K.-A. *Dalton Trans.* **2003**, 4356−4366. (b) Antes, I.; Frenking, G. *Organometallics* **1995**, *14*, 4263−4268.

(14) (a) Becke, A. D. *Phys. Rev. A* **1988**, *38*, 3098−3100. (b) Perdew, J. P. *Phys. Rev. B* **1986**, *33*, 8822−8824.

(15) Zhao, Y.; Schultz, N. E.; Truhlar, D. G. *J. Chem. Phys.* **2005**, *123*, 161103−161107.

(16) (a) Becke, A. D. *J. Chem. Phys.* **1993**, *98*, 5648−5652. (b) Lee, C.; Yang, W.; Parr, R. *Phys. Rev. B* **1988**, *37*, 785−789.

(17) Perdew, J. P.; Burke, K.; Ernzerhof, M. *Phys. Rev. Lett.* **1996**, *77*, 3865−3868.

(18) Mondal, K. C.; Roesky, H. W.; Schwarzer, M. C.; Frenking, G.; Tkach, I.; Wolf, H.; Kratzert, D.; Herbst-Irmer, R.; Niepötter, B.; Stalke, D. *Angew. Chem.* **2013**, *125*, 1845−1850; *Angew. Chem., Int. Ed.* **2013**, *52*, 1801−1805.

(19) *APEX2*, *SAINT*, and *SHELXTL*; Bruker AXS Inc.: Madison, WI, 2009.

(20) Sheldrick, G. M. *SADABS*; University of Göttingen: Göttingen, Germany, 2009.

(21) Sheldrick, G. M. *Acta Crystallogr.* **2008**, *A 64*, 112−122.

(22) Hübschle, C.; Sheldrick, G. M.; Dittrich, B. *J. Appl. Crystallogr.* **2011**, *44*, 1281−1284.

(23) Schäfer, A.; Horn, H.; Ahlrichs, R. *J. Chem. Phys.* **1992**, *97*, 2571−2577.

(24) Ahlrichs, R. *Phys. Chem. Chem. Phys.* **2004**, *6*, 5119−5121.

(25) (a) Deglmann, P.; Furche, F. *J. Chem. Phys.* **2002**, *117*, 9535−9538. (b) Deglmann, P.; Furche, F.; Ahlrichs, R. *Chem. Phys. Lett.* **2002**, *362*, 511−518. (c) Deglmann, P.; May, K.; Furche, F.; Ahlrichs, R. *Chem. Phys. Lett.* **2004**, *384*, 103−107.

(26) Weigend, F.; Häser, M.; Patzelt, H.; Ahlrichs, R. *Chem. Phys. Lett.* **1998**, *294*, 143−152.

(27) Frisch, M. J.; et al. *Gaussian09*, Revision C.1; Gaussian, Inc.: Wallingford, CT, 2010.
(28) Ahlrichs, R.; Bär, M.; Häser, M.; Horn, H.; Kölmel, C. *Chem. Phys. Lett.* **1989**, *162*, 165−169.